

1 Alessandra Marini, Andrea Belleri, Marco Preti, Paolo Riva, Ezio Giuriani. 2017. "Lightweight
2 extrados restraining elements for the anti-seismic retrofit of single leaf vaults". Engineering
3 Structures, Vol. 141, pp. 543-554. DOI:10.1016/j.engstruct.2017.03.038

4
5 **Publisher's version:**

6 <http://dx.doi.org/10.1016/j.engstruct.2017.03.038>

7
8
9 **Lightweight extrados restraining elements for the anti-seismic retrofit of**
10 **single leaf vaults**

11 *Alessandra Marini¹, Andrea Belleri², Marco Preti³, Paolo Riva⁴, Ezio Giuriani⁵*

12 **Abstract**

13 Substantial vulnerability of single-leaf vaults has repeatedly been observed in the aftermath of past
14 earthquakes. Major vault damage or even collapse may follow the onset of mechanisms such as the indirect
15 bending of the vault crown caused by the unconstrained rocking of the abutments, the shear failure of the
16 vault lunettes induced by possible differential rocking of the supporting masonries, and the direct
17 differential bending induced by the inertia forces acting as a uniformly distributed horizontal load along the
18 vault crown. Unlike other mechanisms, which can be inhibited by traditional global retrofit interventions
19 aimed at triggering a box-like seismic response of the existing building, limiting direct bending requires
20 targeted measures on the vault crown. In this paper, extrados lightweight plywood restraining structures
21 applying passive confinement actions are conceived to delay the onset of the vault direct bending failure
22 mechanism. The reinforcement is designed as a 3-hinged arch, hinged-constrained at the springing and at
23 the vault key section to enable small relative displacements of the vault springing, which may follow the

¹ Associate Professor, University of Bergamo, alessandra.marini@unibg.it

² Assistant Professor, University of Bergamo, andrea.belleri@unibg.it

³ Assistant Professor, University of Brescia, marco.preti@unibs.it

⁴ Full Professor, University of Bergamo, paolo.riva@unibg.it

⁵ Full Professor, University of Brescia, ezio.giuriani@unibs.it

24 deformation of any internal ties or roof box structure. The technique is a lightweight and dry solution that
25 does not require specialised labour; it is reversible and minimally impairs the structure's integrity, thus
26 respecting major restoration principles. The effectiveness of the solution is verified through an
27 experimental study on the behaviour of a strengthened single-leaf vault, also in the case of possible relative
28 displacements of the abutments. A special pivoting testing frame is conceived to apply cyclic, uniformly
29 distributed inertia-like forces. The strengthened vault is shown to substantially outperform the response of
30 an unreinforced single leaf vault, tested in a previous research study.

31 *keywords: single-leaf vault; seismic vulnerability; direct bending; local mechanism, strengthening; passive*
32 *confinement; restraining structure; extrados technique; plywood structure.*

33 **1. Introduction and research significance**

34 Single leaf vaults, which are widespread over the Italian and southern European territory, are thin vaults
35 (about 50mm thick) made of a single layer of flat laid bricks, either running longitudinally or in a
36 herringbone brick pattern (Fig. 1) [1],[2],[3]. Often adopted in residential and religious buildings, single leaf
37 vaults are usually shaped as barrel, groin, and pavilion vaults and may bridge spans ranging between 3 and
38 10m (3 ÷ 6m in residential buildings; 6 ÷ 10m as vaulting covering the main nave in religious buildings, [4]).

39 When adopted as walkable horizontal partitions in residential buildings, they usually feature extrados filling
40 material, such as tightly packed rubbles or lunettes overlaid by the finishing pavement tiles. Backfill
41 material or lunettes provide a stabilizing contribution [5]. On the other hand, in the most frequent
42 applications, such as in churches, single leaf vaults lack any filling material and basically behave like
43 lightweight false ceilings solely withstanding their self-weight. Unlike heavier masonry vaults that require a
44 significant vertical stabilising load and are usually located on the building's ground floor, false ceiling single
45 leaf vaults may also be located at the upper levels of traditional masonry buildings.

46 The **equilibrium** of masonry single leaf barrel vaults is guaranteed as long as the thrust line, associated with
47 both static and seismic loads, lies within the vault thickness [6, 7, 8, 4, 9]. In single-leaf vaults the thrust line
48 has a reduced possibility to shift and change within the small vault thickness in order to adapt to different

49 unsymmetrical load distributions [4, 10, 11], or possible spreading of the supports [12], unless lunettes or
50 spandrel walls strengthen the vault extrados against bending actions. In the case of plain single leaf vaults,
51 the maximum shift can be attained if the structure has a catenary geometry, i.e. if the thrust line overlays
52 the centroid axis; conversely, in the case of circular geometry, the possibility to shift is further reduced. As a
53 result, these structures are particularly vulnerable even to low intensity earthquakes. Their extreme
54 vulnerability has repeatedly been assessed after recent earthquakes, when a significant number of single-
55 leaf vaults collapsed, regardless of the earthquake intensity and of the level of the global damage to the
56 structure [13].

57 In the case of a **seismic event**, thin single-leaf vaults can undergo three main mechanisms, namely: (a)
58 indirect differential bending; (b) severe shear distortion; (c) direct differential bending [13].

59 **Indirect differential bending** follows an unconstrained rocking motion of the abutment or supporting wall,
60 which in turn induces the rotation of the vault supports (Figure 2a). Such rotations force differential
61 bending along the vault crown. In the case of either out-of-phase rocking or differential drift of the
62 perimeter walls, the relative displacement of the vault springing can also worsen the indirect bending of
63 the vault crown. Interestingly, indirect bending can be limited or inhibited through global interventions,
64 such as roof or floor diaphragms, aimed at constraining or reducing the rotation or relative displacement of
65 the vault springing.

66 **Severe shear stresses and distortion** follow the onset of differential rocking along the nave ends.
67 Differential rocking occurs as a result of the difference in stiffness between the façade and the transverse
68 arches [13, 14] (Figure 2b). The differential rocking mechanism can be inhibited or confined by adopting a
69 stiff roof box-structure constraining the perimeter masonries along the edge and limiting the possible shear
70 distortion [15].

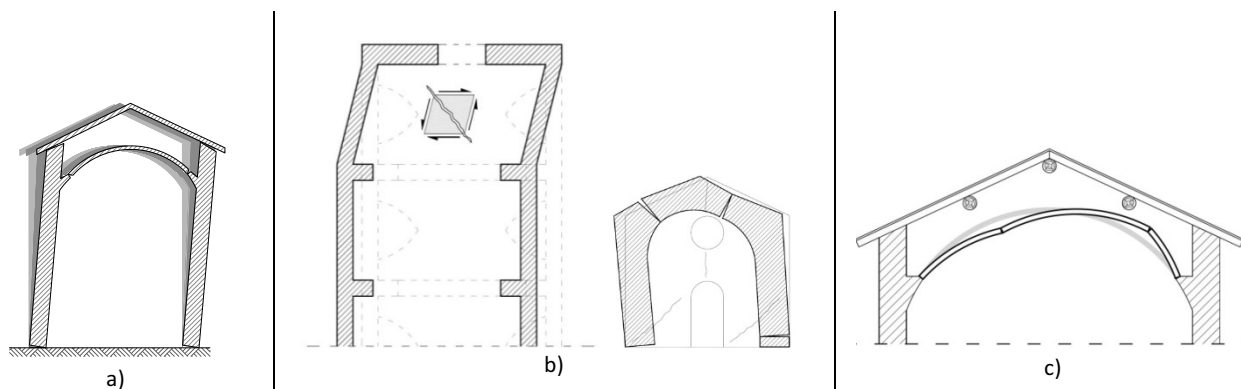
71 **Direct differential bending** is the result of the distributed seismic actions associated with the vault mass.
72 Depending on the earthquake magnitude and the vault thickness, direct bending can be as severe as to
73 cause the structure to collapse, characterised by the onset of a four hinge mechanism [14, 16, 17, 18]

74 (Figure 2c). Past experimental and theoretical studies have ascertained the vulnerability of single leaf vaults
75 with respect to direct differential bending [19]. Practical abaci for the evaluation of the vault collapse
76 multiplier as a function of the main geometry characteristics were provided, and single leaf vault collapse
77 was assessed to be triggered by moderate to low seismic actions, corresponding to horizontal accelerations
78 ranging between $0.04g \div 0.10g$. It is worth noting that, unlike other failure modes, and regardless of the
79 global mitigation measures reducing the vulnerability of the whole building, this mechanism cannot be
80 inhibited, unless special targeted interventions are carried out on the structural element.



Figure 1. Typical single leaf vault with herringbone brick pattern.

81
82
83
84



85 Figure 2. Main vulnerabilities of single leaf vaults undergoing seismic actions: (a) indirect bending following rocking of the
86 abutments; (b) shear distortion following differential rocking; (c) direct bending of the vault subject to the seismic action associated
87 with its own mass. In the proposed strengthening approach a) and b) are considered as inhibited by global strengthening of the
88 structure with roof box structures and focus is placed on the direct bending mechanism of the sole vault.
89

90 In order to upgrade the seismic resistance of single leaf vaults, the **traditional techniques developed for**
91 **the strengthening of masonry vaulted structures are usually addressed**. Some adjustments are needed to
92 account for the reduced thickness of these particular kinds of vaults. For example, attention must be paid
93 to avoid a significant increase in dead load, which in turn could result in additional seismic actions
94 anticipating failure; also, care must be paid so as to avoid unsymmetrical load sets.

95 Among the possible techniques **masonry spandrel walls** [14, 16, 20, 21], are worth mentioning. Spandrel
96 walls are extrados retaining structures conceived to either constrain the deformation of the vault crown, or
97 enforce a composite structure behaviour that allows the thrust line to migrate within the spandrel wall
98 height. This intervention allows the substitution of the stabilising backfill material with possible reduction
99 of the vault mass. As a main drawback, in the case of partial spandrel walls, which do not extend up to the
100 vault key, problems may arise in the case of relative displacements of the springing.

101 The seismic retrofit can also be obtained through thin **RC extrados slabs**, which are usually secured to the
102 vault ring through either studs, special devices, or by relying on friction so as to enable shear transfer along
103 the vault-to-reinforcement interface. The resistance of the structure is therefore increased by enforcing a
104 composite structure behaviour, increasing the thickness of the vault, thus allowing the ideal resisting arch
105 to adjust within a higher thickness. The solution strengthens the vault with respect to both symmetrical and
106 unsymmetrical load sets, but nowadays it is discarded as the concrete may induce chemical incompatibility
107 with the masonry. The use of thin **high performance natural lime mortars strengthened with inorganic**
108 **fibre mesh** can be regarded as an enhancement of the previous technique, ensuring chemical and
109 mechanical compatibility [22]. As a major drawback, regardless of the material adopted, the vault mass
110 increases and this may be impairing for single leaf vaults. More importantly, in the case of effective slab-
111 vault composite behaviour, the thrust line might migrate in the overlaying slab over time, inducing the
112 possible decompression of the vault crown. Such a situation could be detrimental in seismic conditions,
113 entailing the risk of debonding and unthreading of bricks from the existing structure [16].

114 The use of **fibre-reinforced polymer strips (FRP)** has been also proposed [23]. It has been demonstrated
115 that FRP retrofit enhances vault strength and ductility by inhibiting the 4 hinge mechanism. Failure of the
116 strengthened structure may arise due to possible shear failure close to the springing as the technique
117 enhances the sole bending capacity, while leaving shear strength unchanged [23]. The width of the strips
118 was shown to affect the ultimate strength of the retrofitted structure. Delamination of the FRP strips may
119 also govern structural collapse, and may be triggered either by the uneven surface of the vault or by failure
120 of the bond between the vault and the laminate. Ultimately, loss of transpiration potential may accelerate

121 local decay processes over time and durability issues may arise as the binding material has not been tested
122 against aging. The use of either steel-reinforced grouts (SRG) [24], or inorganic matrix grids (IMG)
123 embedded in lime-based mortar can be regarded as an alternative to this technique, increasing durability of
124 the intervention [25, 26].

125 **Intrados and extrados steel ties** are usually adopted to withstand the lateral thrust of the vault and to
126 reduce possible relative displacements of the abutment at the level of the vault impost. This technique
127 does not affect the direct bending behaviour of the vault.

128 **Lightweight ribs** overlaying the vault extrados profile may also reduce vulnerability with respect to direct
129 bending [18]. The ribbed tubular cross section is made of lime mortar reinforced with inorganic matrix
130 grids; the inner lightweight core is made of polystyrene elements. No shear transfer is allowed along the
131 vault-to-rib interface in order to prevent or limit decompression of the vault. This way, the vault self
132 supports its dead load and the static behaviour is unaltered in service conditions; whereas in the case of an
133 earthquake, the lightweight rib constrains the vault deformations, thus providing passive confinement.

134 In this paper, a new strengthening technique for the reduction of the seismic vulnerability of single-leaf
135 vaults against direct differential bending is presented. **Extrados stiff lightweight plywood restraining**
136 **structures** (resembling extrados centering and referred to as “centering” or “restraining structure” in the
137 following) that apply passive confinement are specifically conceived to delay the onset of the 4-hinge
138 failure mechanism of the single leaf vault. The proposed technique is a passive solution, maintaining the
139 structural role of the vault and providing confinement only if needed. It is a lightweight, dry and cost-
140 effective solution, whose assembly and positioning does not require any specialised labour. The solution is
141 conceived as fully reversible and minimally impairing of the structure’s integrity, thus it respects strict
142 conservation principles.

143 The extrados reinforcement is designed as a **3-hinged arch**, hinged at the abutments and with an internal
144 hinge at the vault key section; such a structural scheme allows the accommodation of small relative
145 displacements of the vault springing following the deformation of any internal ties or roof box structure.

146 The centering simply overlays the existing vault extrados. **No shear transfer** is allowed along the vault-to-
147 centering interface in order to prevent or limit the decompression of the vault. This way, in static
148 conditions, the vault self-supports its dead load and maintains the original compression state. In seismic
149 conditions, the lightweight restraining structure provides passive confinement by limiting vault
150 deformations.

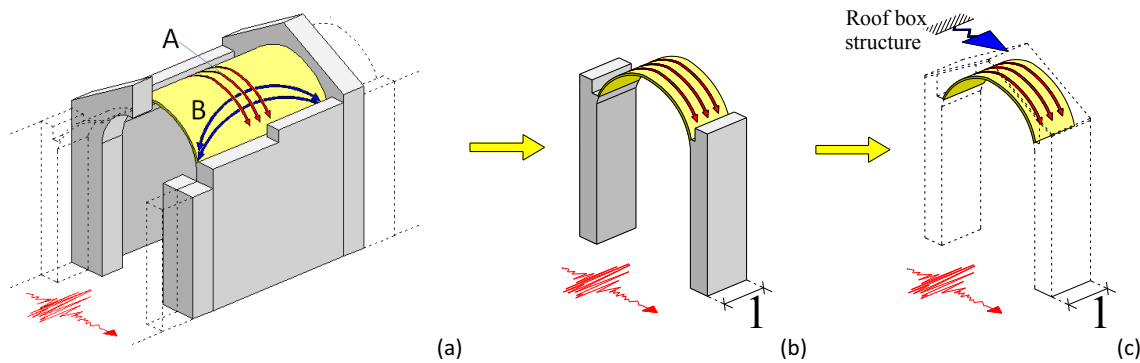
151 The effectiveness of the solution is assessed through an **experimental study** on the behaviour of a
152 strengthened single-leaf vault subjected to cyclic, distributed unsymmetrical loads. The performance of the
153 strengthened vault is then compared to the seismic response of a reference unreinforced single leaf vault,
154 tested in a past research study [19, 27, 28]. Finally, reliability of the solution is further verified in the case of
155 possible small relative displacements of the supports, such as those allowed by compatible elongation of
156 intrados ties.

157 **2. Framework of the study and modelling of the reference structure**

158 The basic hypotheses establishing the framework of the study are described below. Reference is made to
159 the strengthening of the **traditional single leaf barrel vault typology, lacking the backfill material**, which
160 can be commonly found either in churches or in the upper floors of residential buildings, where single leaf
161 vaults serve as false ceilings.

162 The single leaf vault is modelled as a **series of transverse adjoining vault stripes** ("A" in Fig.3a). This
163 assumption simplifies the actual tridimensional structural behaviour, which should more accurately account
164 for the longitudinal natural arches developing between the head walls or transverse arches ("B" in Fig.3a).
165 These longitudinal arches strengthen the structure by laterally confining the transverse vault stripes. In the
166 following, the beneficial tridimensional confining effects are neglected and reference is made to a **single**
167 **barrel vault stripe of unit width** (Fig.3b). Given that the main objective of the analysis is the design of an
168 appropriate vault strengthening solution, the assumption of neglecting the tridimensional resisting
169 contribution is conservative and thus on the safe-side.

170 It is assumed that both indirect bending and shear distortion are either substantially limited or inhibited
 171 through global interventions such as roof diaphragms or perimeter ties, and reference is made to the case
 172 of a **vault undergoing direct bending only** (see the nonlinear spring support at the roof ridge line modelling
 173 the stiffness and strength of the roof box structure in Fig.3c) [15]. Based on this assumption, the sole vault
 174 is modelled in the experimental specimen, and the vault supports are assumed as fixed to the testing bench
 175 (Fig.3c). To accurately represent **direct bending conditions**, both distributed vertical loads modelling the
 176 dead load and distributed horizontal loads representing the seismic action pertaining to the vault are
 177 considered. Possible small relative displacements of the springing are also considered.



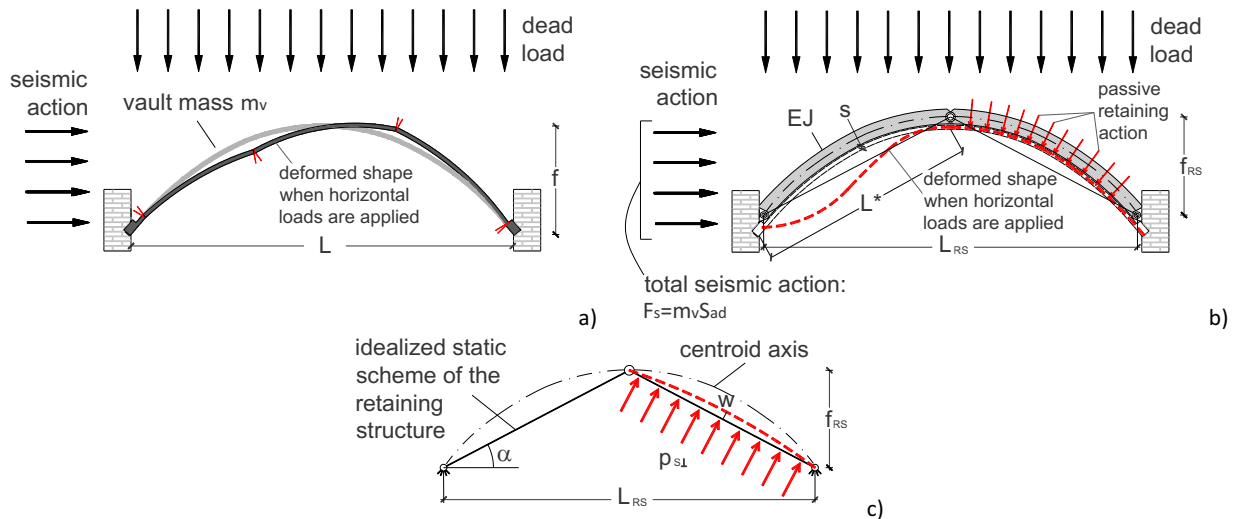
178
 179 Figure 3. Modelling steps for the design of the experimental specimen: (a) Tridimensional structural behaviour of a single-leaf vault,
 180 developing transverse (A) and longitudinal (B) resisting arches; (b) simplified modelling of the vault behaviour as a series of
 181 adjoining vault stripes of unit width; (c) focus on the vault ring in the assumption that a roof box structure avoids or significantly
 182 limits the abutment rocking mechanisms.

183 2.a Single leaf barrel vault experimental specimen

184 Based on these assumptions, the experimental masonry vault specimen is a basic single-leaf barrel vault
 185 stripe of unit width (span $L=5m$, rise $f=1.42m$, thickness $t=52mm$); neither backfill material nor lunettes,
 186 providing stabilising contribution, are considered. The single-leaf barrel vault stripe has a polycentric
 187 profile, with the geometric mid axis line approximately overlapping the thrust line associated with self-
 188 weight loads.

189

190 **Flat brick arrangement with a running bond masonry texture is considered.** In the running bond pattern,
191 cohesion of the brick-mortar interface is negligible and does not provide a significant contribution to
192 resistance. The binding lime mortar mix design is calibrated to replicate the mechanical characteristics of
193 historical brick masonries. **Material characterisation** tests were performed on specimens prepared during
194 the construction of the vault and the main material properties are listed in Table 1 (further details in [19,
195 28]). The vault stripe is embedded at the springings and subject to uniformly distributed vertical and
196 horizontal loads. The expected collapse mechanism for the unstrengthened vault is characterised by the
197 onset of four plastic hinges (Fig.4a). The assembled specimen is shown in Figure 5a.



198

199

200

201

202

203

204

205

206

207

Figure 4. a) Four hinge mechanism of the bare single leaf vault induced by direct differential bending collapse mechanism, triggered by the distributed seismic actions associated with the vault mass; b) extrados 3-hinge retaining structure applying passive confinement actions to the vault extrados; c) idealised static scheme of the retaining structure as a 3-hinge arch undergoing uniformly distributed load on the leeward beam.

Table 1. Average mechanical properties of brick units, mortar, masonry and plywood panels

| Solid Clay Brick [data provided by the supplier] | | |
|---|--------|-------------------|
| Young's modulus | ~ 8000 | MPa |
| Poisson's coefficient | 0.15 | - |
| Weight density | ~ 17 | kN/m ³ |
| Horiz. compressive strength | > 6 | MPa |
| Mortar [NHL: 7.5% - Lime putty: 8.5% - Aggregates 1.5mm: 34% - Aggregates 3mm: 34% - H2O: 16%] | | |
| Young's modulus | 661 | MPa |
| Weight density | ~ 21 | kN/m ³ |
| Compressive strength | 1.87 | MPa |
| Tensile strength | 0.20 | MPa |
| Masonry | | |
| Initial Young's modulus | 4006 | MPa |
| Initial Poisson's coefficient | 0.10 | - |
| Weight density | ~ 18 | kN/m ³ |
| Compressive strength | 3.37 | MPa |
| Tensile strength | 0.07 | MPa |
| Brick-to-mortar interface cohesion | 0.04 | MPa |
| Brick-to-mortar interface initial friction angle | 29.25 | ° |
| Brick-to-mortar interface residual friction angle | 28.36 | ° |
| Plywood Panels | | |
| Young's modulus | > 4000 | MPa |
| In-plane flexural strength | > 40 | MPa |
| Poisson coefficient | 0.3 | |
| density | 13.8 | Kg/m ² |

208

209 2.b Extrados lightweight restraining structure

210 The single leaf vault specimen stripe is strengthened against direct differential bending mechanism by
211 means of **two lightweight restraining structures**, pinned to the abutments, applying passive confinement
212 to the vault extrados (Figure 4b). In static conditions the vault is subjected to the self-weight without
213 interfering with the restraining structures, whereas in seismic conditions the vault is contained by the
214 restraining structure. The leeward portion of the vault is confined and only the windward part, having
215 approximately half of the initial span (L^* in Fig. 4b), can undergo the four hinge mechanism. As a result the
216 seismic vulnerability is significantly reduced.

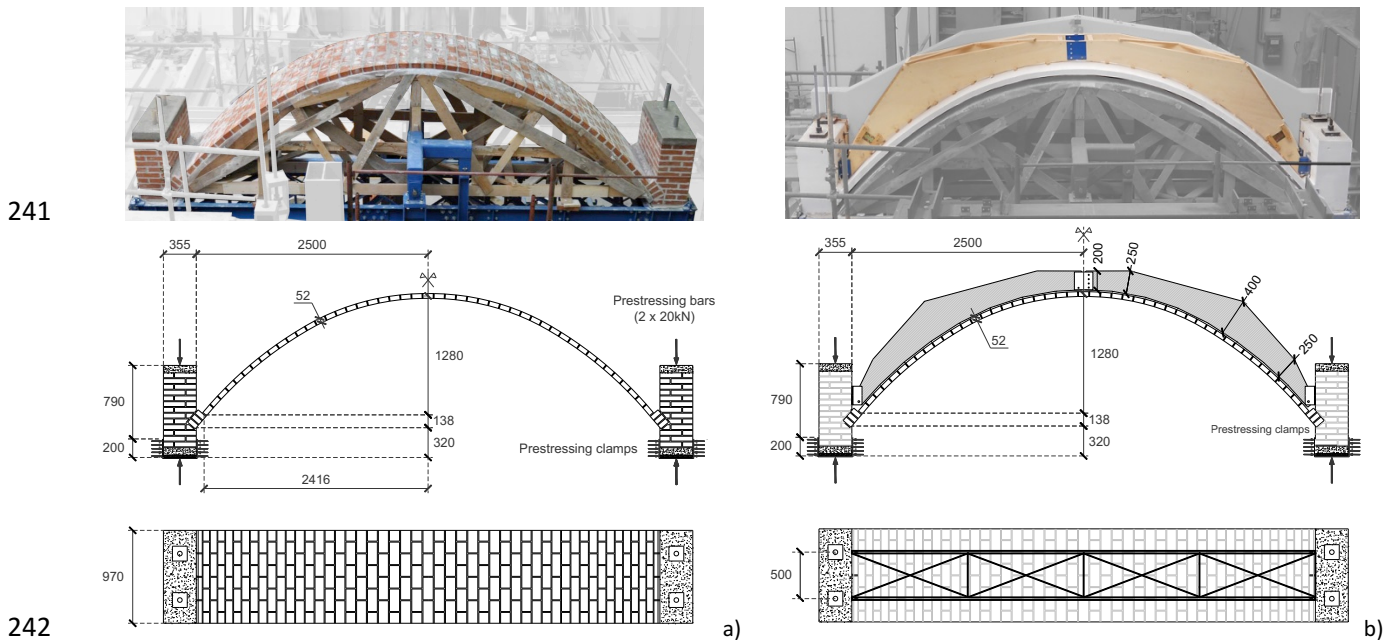
217 The extrados reinforcement is designed as a **3-hinged arch**, hinged-constrained at the masonry abutments
218 by the vault supports, and at the mid-span, by the vault key section. Such a hinge location allows for small
219 relative displacements of the abutments at the vault springings. Note that no in-plane shear distortion of
220 the vault is considered given the hypothesis of roof diaphragm, inhibiting any relative displacement of the
221 abutments in the direction parallel to the extrusion line of the vault. Furthermore, the hinges at the
222 springing and at the vault key are located below the centering centroid axis, as close as possible to the
223 extrados of the vault (Fig.5b and Fig. 6). Such a hinge location minimises the distance between the vault
224 centroid axis and the centering. This in turn reduces the relative displacements of the two structures in the
225 case of either unsymmetrical load conditions (such as in the case of an earthquake) or in the case of
226 spreading supports, thereby limiting the impairment caused by dynamic impacts induced by actual seismic
227 loadings.

228 Given the low self-weight of the considered type of single leaf vault, inertia forces are indeed very small
229 and fairly “light” strengthening structures are effective in delaying the onset of a possible failure
230 mechanism. For the **proportioning** of the cross section of the restraining structure, for the sake of simplicity
231 and on the safe side, the total design horizontal inertia forces pertaining to single leaf vault ($F_s = m_v S_{ad}$, where
232 m_v is the vault mass and S_{ad} is the pseudo acceleration at the vault springing, Fig. 4b) can be preliminarily
233 assumed to be loaded onto the strengthening structure, which is idealised as a 3-hinge arch undergoing

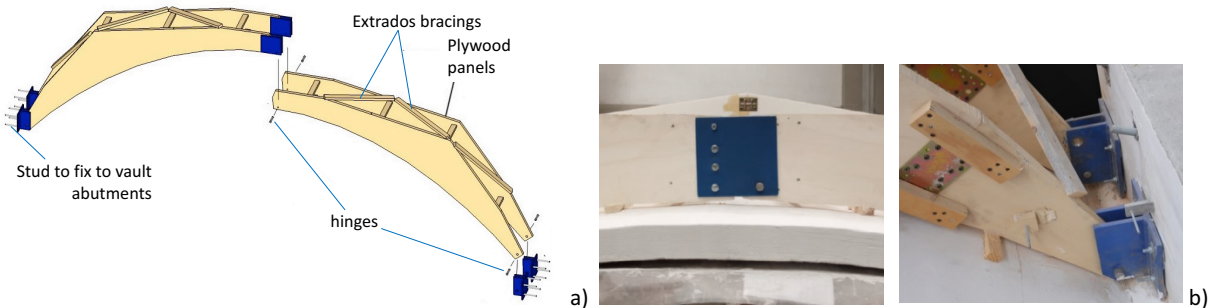
234 uniformly distributed actions along the leeward beam ($p_s = F_s/L^*$, where $L^* = 0.5L_{RS}/\cos\alpha$ and $\tan\alpha = 2f_{RS}/L_{RS}$,
 235 Fig. 4c). The restraining structure can be designed by enforcing that the maximum deflection (w) of the
 236 leeward beam be sufficiently smaller than the vault thickness (s), i.e. $w < \beta s$ with β possibly ranging
 237 between $1/100 \div 1/500$. With reference to Figure 6b the preliminary value of the flexural stiffness of the
 238 strengthening structure can be obtained:

239
$$EJ > \frac{5p_{s\perp}L^{*4}}{384\beta s}$$

240 where $p_{s\perp} = p_s / \sin\alpha$.



242
 243 Figure 5. Side view and geometry of a) the bare vault stripe and b) of the strengthened vault with extrados 3-hinge wooden
 244 centering.
 245



247 Figure 6. Detail of the centering components and of the hinge location. Wooden wedges forcing contact between the vault and the
 248 retaining structure are displayed in b) and c).
 249

250 In the experimental test, two restraining structures made of 30mm thick plywood panels, braced together
 251 along the extrados edge to avoid buckling, are proposed (Figures 5b and 6). Assuming both $\beta = 1/200$ and an

252 acceleration equal to 0.5g, by considering $s = 50\text{mm}$, $E = 4000\text{ MPa}$, $L^* = 2.66\text{ m}$, $\alpha = 27^\circ$, $p_{s\perp} = 0.5 \cdot$
253 $(0.05\text{m} \cdot 1.0\text{m} \cdot 18\text{kN/m}^3) / \sin\alpha = 1\text{kN/m}$, it yields: $J \geq 3.26 \cdot 10^8 \text{mm}^4$, corresponding to two elements of
254 400mm in height (assuming constant cross-section for each element).

255 It is worth noting that other materials could have been used as long as stiff and lightweight restraining
256 structures, with the envisioned 3-hinge static scheme, were obtained. Therefore either steel, GFRP or
257 wooden truss-works, XLAM panels, etc. could have been used instead. The side view and geometry of the
258 strengthened structure are shown in Figure 5b. Initial contact between the centering and the vault is
259 enforced through thin wooden wedges (Fig.6), whereas no shear transfer is allowed along the vault-to-
260 centering interface, except for the minor friction at the wedges, in order to prevent or limit possible vault
261 decompression. Alternatively, a thin layer of mortar could be used to enable initial contact, whilst friction
262 along the interface may be inhibited through interposition of a thin cellophane sheet.

263 **3. Experimental test set-up**

264 A special swinging testing bench, which was conceived during a past research program aimed at assessing
265 the seismic vulnerability of single leaf vaults, was used [27]. The testing bench was conceived to impose
266 uniform horizontal acceleration; the inertia forces along the vault crown are replicated by equivalent quasi-
267 static uniformly distributed forces, whereas no dynamic effects are taken into account (details are
268 summarised later, and further discussed in [19]). The testing bench is made of a rigid steel deck hanging
269 from a vertical frame fixed to the ground (Fig. 7a). The steel deck rigidly rotates both clockwise and
270 counter-clockwise about a pivot point A. Deck rotations are induced through a mechanical transmission
271 system, actuated by an electromechanical jack.

272 The specimen was assembled on the steel deck. Pre-stressing clamps and anchoring bars were installed to
273 fix the vault abutments to the deck to avoid their possible relative rotation. This way, the load distribution
274 following the rotation of the deck can involve only the direct differential bending mechanism of the vault
275 ring.

276 For increasing the tilting angle of the deck (θ), increasing distributed relative horizontal loads act on the
 277 vault ring: in the tilted position, the gravity acceleration (g) can be decomposed, with respect to the
 278 specimen tilted local axes (x,y), into two orthogonal vectors, resulting in both vertical $a_y(\theta)=g\cdot\cos\theta$ and
 279 horizontal $a_x(\theta)=g\cdot\sin\theta$ relative accelerations applied to the vault ring (Fig.7a). For each deck tilting
 280 angle, the horizontal-to-vertical acceleration ratio $\alpha(\theta)$ can be defined as:

281
$$\alpha(\theta) = \frac{a_x(\theta)}{a_y(\theta)} = \frac{g \cdot \sin\theta}{g \cdot \cos\theta} = \tan\theta$$

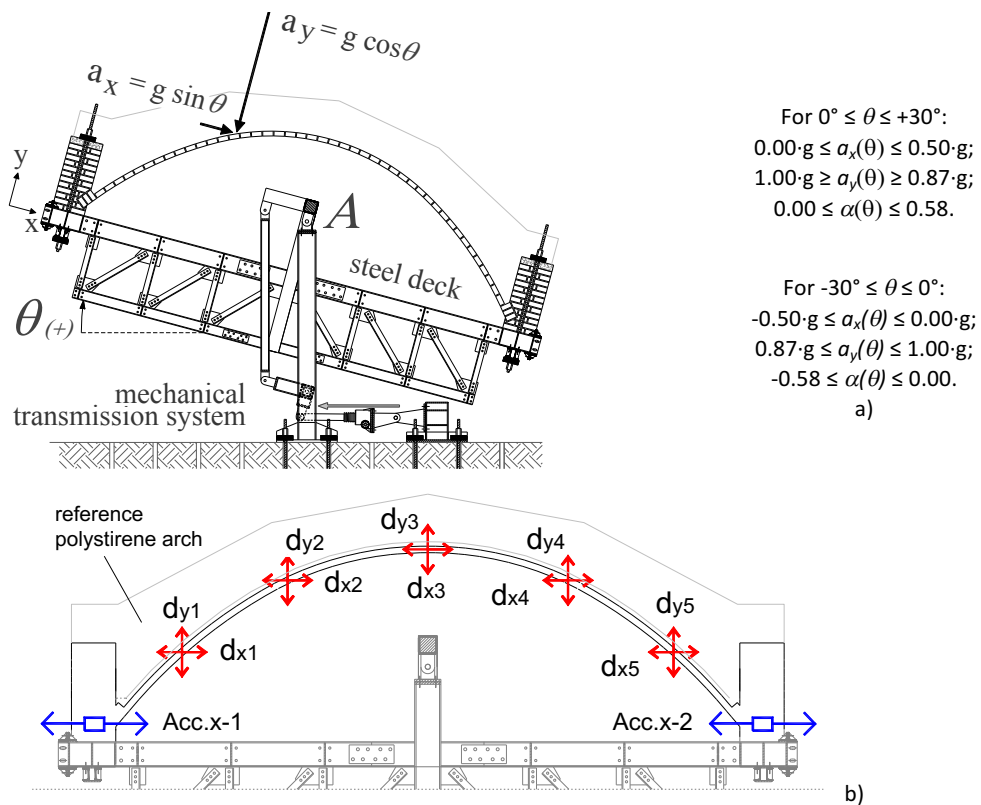


Figure 7. a) View of the swinging testing frame: in the tilted position, the gravity acceleration is decomposed into two components of horizontal $a_x(\theta)$ and vertical $a_y(\theta)$ relative accelerations; clockwise and counter-clockwise maximum rotations and extreme values of relative accelerations and horizontal-to-vertical acceleration ratio are shown; b) instruments set-up.

282

283 The horizontal acceleration component in the tilted local reference axis system $a_x(\theta)$, replicating distributed
 284 seismic acceleration, ranges between 0 and 0.5g for deck tilting angles approaching the maximum testing
 285 frame rotation capacity, equal to $\pm 30^\circ$. Unlike seismic conditions, in which the dead loads are kept
 286 constant and the sole horizontal loads replicating the earthquake actions are varied, in the experimental

287 tests the relative vertical acceleration component $a_v(\theta)$ slightly reduces for increasing values of the tilting
288 angle θ . Specifically, the vertical load reduction ranges between 0 and 13.4% for tilting angles varying
289 between 0° and 30° degrees. In the case of unstrengthened single-leaf vaults, in which collapse is triggered
290 at very small tilting angles [27], the vertical load variation is negligible. In the case of strengthened vaults,
291 the variations of the vertical component of the load could be more significant, being at most equal to
292 13.4%.

293 It is worth noting that, although the electromechanical jack is operated with displacement-control, the
294 experimental test is carried out in load-control. The rotation imposed to the steel deck corresponds to a
295 relative acceleration, and thus to a force, acting on the specimen. Accordingly, no evidence of the post-
296 peak behaviour of the vault can be obtained with the conceived experimental test set-up. The post-peak
297 behaviour results in a loss of equilibrium and, consequently, in an uncontrolled accelerated motion of the
298 vault parts. In order to stop the post-peak motion of the vault the wooden formwork adopted for the vault
299 construction was maintained with a gap of 15mm from the vault intrados throughout the test.

300 The vault ring differential deflection was monitored by means of 10 linear variable displacement
301 transducers pinned between the vault mid axis and a rigid polystyrene arch fixed to the specimen
302 abutments (Fig. 7b). The tilting angle of the testing bench was monitored by means of two single-direction
303 accelerometers fixed to the specimen abutments and directed as the relative horizontal axis.

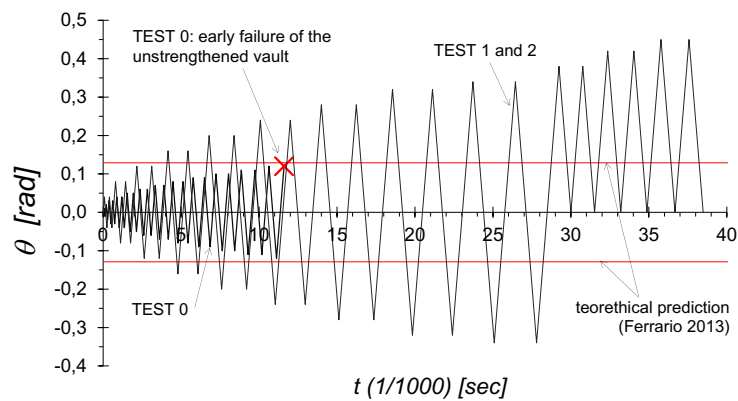
304 By rotating the testing bench, cycles with increasing inclination were imposed to the deck either up to
305 failure or to achieving the maximum rotation capacity of the testing bench ($\theta = \pm 30^\circ = \pm 0.52\text{rad}$).

306 **4. Experimental test results and discussion**

307 Two tests were carried out. In Test 1 the strengthened single leaf vault was subject to uniformly distributed
308 horizontal load cycles of increasing amplitude. In Test 2 the same load history was applied after forcing a
309 relative displacement of the vault abutments, simulating the small elongation of the vault span, which may
310 still occur after the preliminary global intervention enabling the box structure behaviour has been carried

311 out (see chapter 2). Test results were compared with those obtained in a past experimental test carried out
312 on the unstrengthened specimen (Test 0 in the following, Fig. 5a), [19, 27].

313 Test 1 and 2 load histories are presented in Figure 8. Both tests were interrupted due to exceedance of the
314 rotation capacity of the testing frame $\theta = 0.52\text{rad}$, corresponding to a horizontal relative acceleration of
315 about 0.5g. The load history applied to the bare single leaf vault stripe (Test 0) is reported for useful
316 comparison. It is worth noting that the performances of the strengthened specimen substantially exceeded
317 the response of the bare single leaf vault, which showed early failure for $\theta = 0.12\text{rad}$ in Test 0 (red cross).



318
319 Figure 8. Imposed rotation history applied to the unstrengthened (Test 0, solid grey curve; the red cross represents the early failure
320 of the specimen) and to the strengthened specimens (Test 1 and Test 2, solid blue curve: the tests were interrupted due to
321 exceedance of the maximum rotation capacity of the testing bench).
322

323 **Test 1: results and discussion**

324 Test 1 horizontal-to-vertical relative acceleration ratio $\alpha(\theta)$ versus vault horizontal displacement ($d_{x1,2,3}$)
325 curves are shown in Figure 9a and compared to the curve obtained in Test 0 for horizontal displacement
326 (d_{x3}) in Figure 9b.

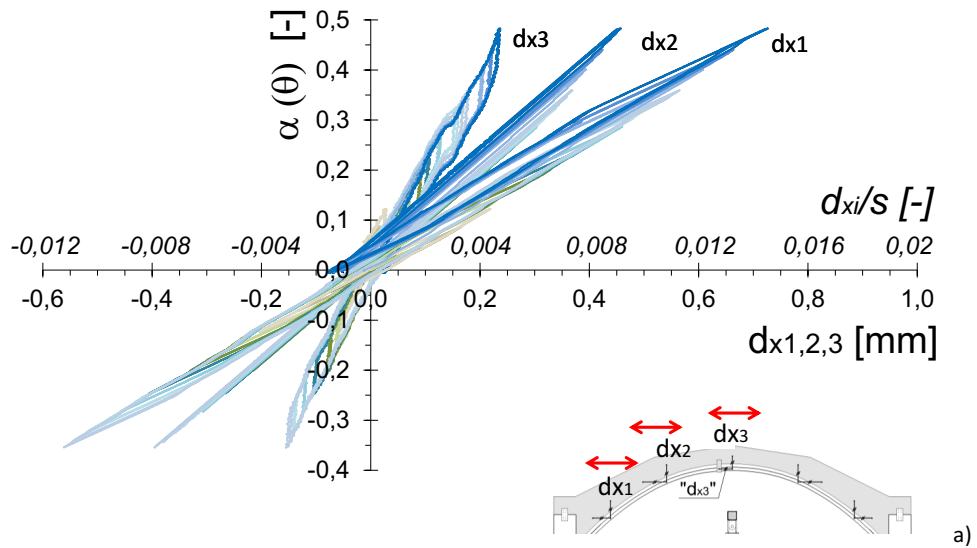
327 During Test 0 the unstrengthened vault exhibited an abrupt loss of stiffness following the development of
328 each new plastic hinge. Unlike in typical masonry macro-block rocking motions, the initial stiffness was not
329 recovered upon load reversal and the expected flag-shape behaviour was not monitored. This was caused
330 by the difference in the “as-built” and the “catenary” profile: the thrust line exceeded the central core of
331 inertia even in the static condition and the cracks did not close upon load reversal, thereby explaining the
332 unrecoverable loss of stiffness.

333 In the strengthened vault the structural behaviour was elastic throughout the test and no onset of
334 kinematic mechanism was observed even for loads 4 times greater than the loads triggering failure in Test 0
335 [29]. LVDTs were removed for horizontal-to-vertical relative acceleration ratio $\alpha(\theta) = 0.48$ and the test was
336 carried out until the rotation capacity of the testing frame was reached (thus for $\alpha(\theta)_{MAX} = 0.58$). The
337 maximum horizontal-to-vertical relative acceleration ratio obtained in Test 1 is quite remarkable and larger
338 than the possible seismic demand associated to the seismic hazard of most of the Italian territory at the life
339 safety limit state, unless the vault would be unrealistically located on quite high floors. It is worth noting
340 that such seismic accelerations are unlikely to be withstood even by retrofitted historical buildings
341 featuring a box-structure behaviour; this means that following the seismic event, thanks to the retrofit, the
342 single leaf vault is expected to no longer be the most vulnerable structural element of the construction.

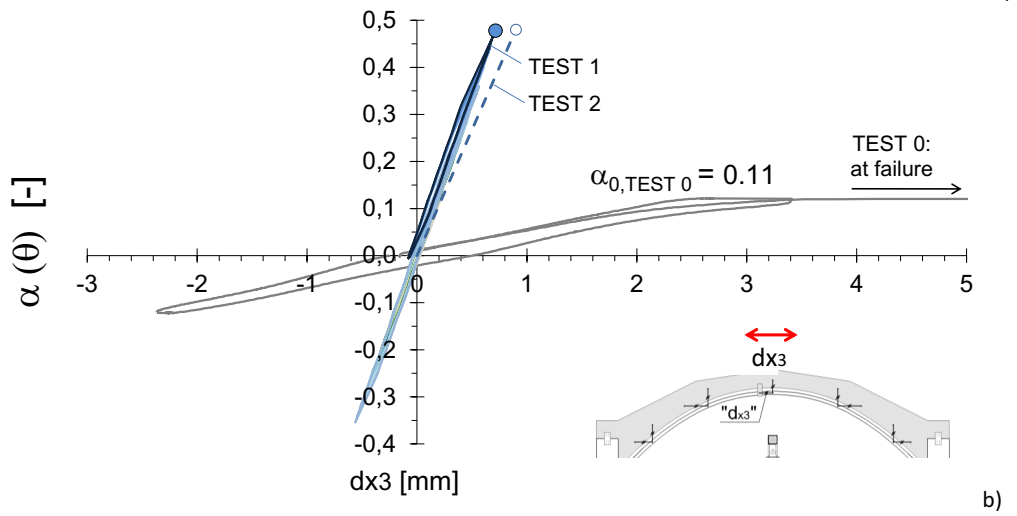
343 Figure 9 also shows that the retrofit remarkably increased the stiffness of the vault, with a consequent
344 reduction of the maximum displacement (d_{x3} was smaller than 1mm in Test 1, whereas it was
345 approximately equal to 3.5mm in Test 0). Such a result is encouraging and coherent with the limited
346 displacement capacity of these structures. In this particular application, reduced displacements are
347 favourable for the conservation of possible stuccos and frescoes often found at the vault intrados. Based on
348 these remarks the proposed technique proved to be an effective solution in increasing the seismic response
349 of single leaf vault.

350 Figure 10 shows the evolution of the deformed shape of the vault induced by the differential deflection
351 following the increasing clockwise rotation in Test 1. The deformed shapes are magnified by 100.
352 Displacements are very small, always smaller than 2 mm, including at tilting angles approaching the
353 rotation capacity of the testing frame. For increasing clockwise rotations, the left part of the vault pushes
354 on the plywood restraining structure, whereas the right part slightly detaches from it; however relative
355 displacements of the restraining structure and the vaults were almost negligible throughout the test. The
356 monitored deformation is coherent with the expected structural behaviour (Fig. 4b). To emphasise the
357 effectiveness of the retrofit in preventing the onset of the differential bending mechanism, the maximum
358 deformation of the unstrengthened vault in Test 0 is also plotted in Figure 10, capturing the deformed

359 shape of the bare vault prior to collapse. Displacements are higher by almost 1 order of magnitude with
360 respect to the displacements measured in Test1. Finally, a side view of the testing apparatus and the vault
361 specimen is shown in Figure 11 for rotations applied approaching the testing frame rotation capacity ($\theta =$
362 $30^\circ \approx 0.52\text{rad}$; $\alpha = -0.58$). No evidence of the onset of failure mechanisms is observed.



363



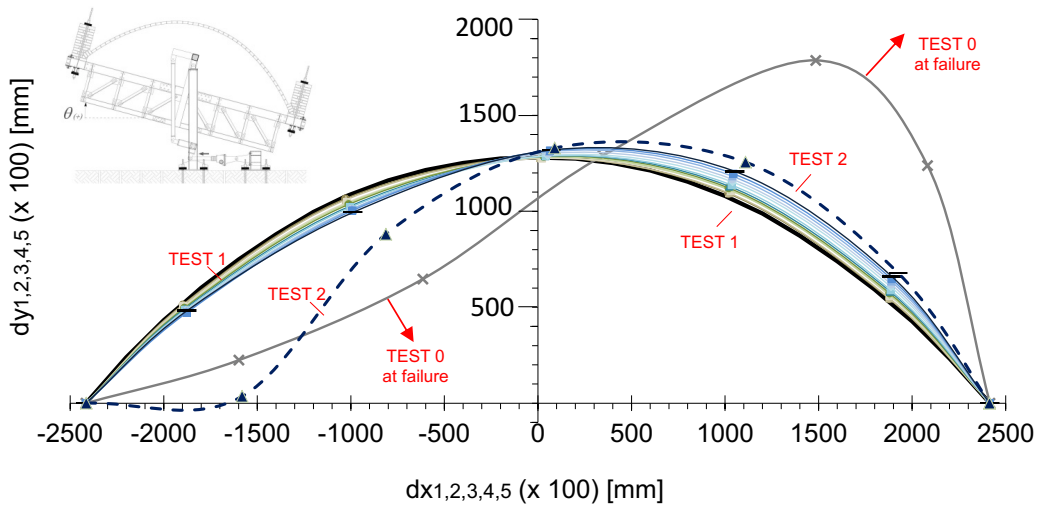
364

365

366

367

Figure 9. a) Horizontal-to-vertical spectral ratio vs horizontal displacement $d_{x1,2,3}$ in Test 1; b) horizontal-to-vertical relative acceleration ratio vs horizontal displacement d_{x3} in Test 0, Test 1 and 2.



368

369

370

Figure 10 - Differential deflection of vault ring for positive tilting angle.

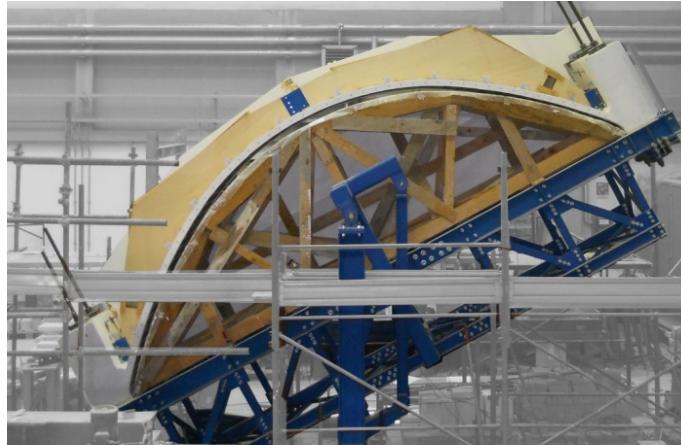


Figure 11 – Side view of the testing apparatus and the vault specimen ($\theta=-30^\circ \approx 0.52\text{rad}$; $\alpha=-0.58$)

371
372
373
374

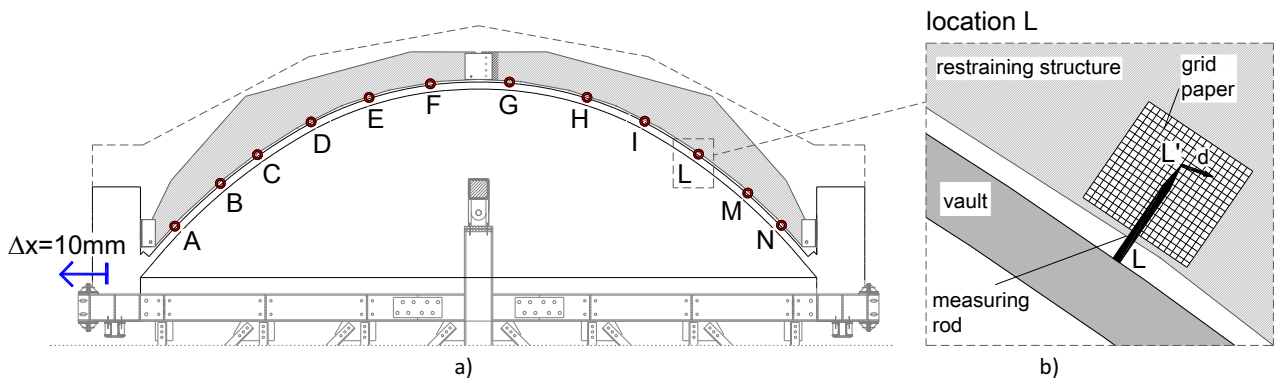
375 **Test 2: results and discussion**

376 In Test 2 a target horizontal settlement $\Delta x=10\text{mm}$ was applied to the left abutment of the vault (Figure
377 12a). The testing bench was modified appropriately, by introducing a bolted device at the deck head, to
378 enable manual application of the envisioned relative displacement of the abutment.

379 It is worth noting that, although the free rocking of the abutment is assumed to be substantially limited by
380 preliminary global interventions (see chapter 2), a minimum elongation of the vault span could still occur as
381 a consequence of either the deformation of the possible transverse ties, or due to the slight out-of-phase
382 rocking of the abutments enabled by the offset between the roof box structure eave-line and the vault
383 springing. In the first scenario, with reference to a vault with a 5m net span, the target settlement
384 replicates the loosening of a tie experiencing a tensile strain of about 2‰, where 2‰ may be assumed as
385 the design strain in the proportioning of new ties, made of good quality steel conceived to withstand
386 tensile actions without yielding. In the second scenario, with reference to a wall height of 5m, the selected
387 Δx may represent a 1‰ out-of-phase drift of the abutments.

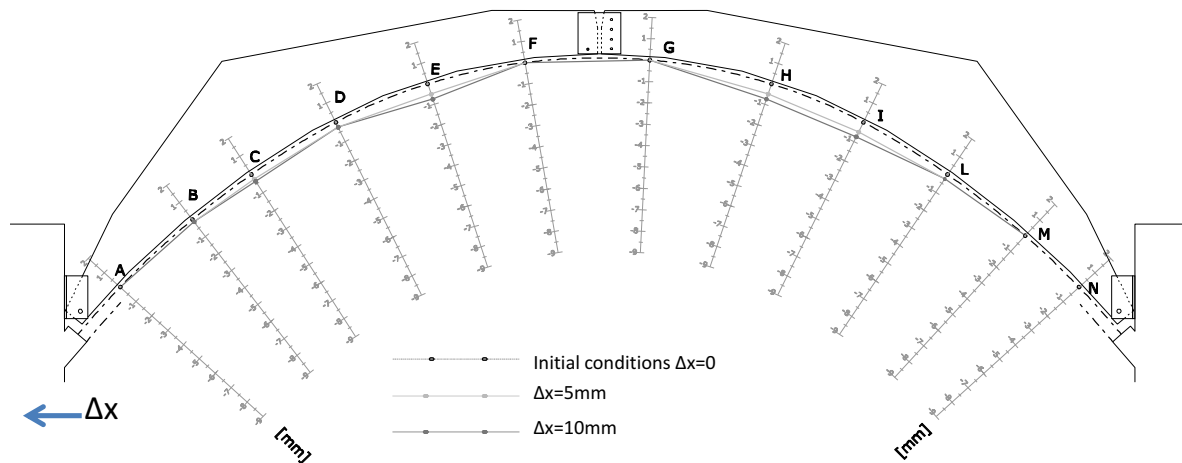
388 In the test, progressive detachment of the plywood restraining structure from the extrados of the vault was
389 monitored for increasing applied settlement at 12 selected locations (A to N in Fig.12a). The relative
390 displacement (d in Fig.12b) of pairs of homologous points (L and L') was measured through miniature

391 measuring rods fixed to the vault extrados and a grid paper glued to the restraining structure side (Fig.
392 12b).



393
394
395
396 Figure 12 – a) Relative horizontal settlement applied to the specimen, and additional instrument set-up monitoring the detachment
397 of the restraining structure from the vault extrados at 12 locations (A to N); b) detail of the measuring rod fixed to the vault
398 extrados and the reference grid paper glued to the restraining structure to capture the possible relative displacement of the
399 homologous points L and L'.
400

401 Figure 13 displays the evolution of the relative displacement for increasing imposed horizontal settlement.
402 As expected, persisting contact of the retaining structure and the vault at the key and springing sections is
403 observed during the settlement application. Provided that the strengthening system is characterised by a
404 reduced rise-to-span ratio with respect to the vault ($F_{RS}/L_{RS} < f/L$, Fig 4), for the given applied horizontal
405 settlement, the restraining structure is expected to undergo slightly larger vertical displacement at the key,
406 thereby maintaining contact with the vault extrados and guaranteeing its restraining action. Along the
407 intermediate sections, the different shape of the two systems causes slight relative detachments, which are
408 symmetrical in relation to the key section and quite small, being at most equal to 0.75 mm in 3 points for
409 the target horizontal displacement of 10mm. The reinforcement 3-hinge static scheme therefore proved to
410 enable small relative displacements of the abutments. Table 2 shows the relative displacements between
411 the restraining structure and the vault extrados after the application of the lateral settlement Δx .



412
 413 Figure 13. Relative displacements between the restraining structure and the vault extrados for increasing the imposed lateral
 414 settlement Δx . Note that the centering is considered as fixed in the undeformed initial shape, whereas it actually undergoes a
 415 kinematic mechanism during the application of the lateral displacement; therefore the diagram does not represent the deformed
 416 shape of the vault but rather the evolution of the relative detachments of the vault and centering system throughout the
 417 application of the lateral displacement (see also Table 2).
 418

419 Table 2. Relative displacements (in mm) between the restraining structure and the vault extrados after the imposed lateral
 420 settlement Δx .

| Δx | A | B | C | D | E | F | G | H | I | L | M | N |
|------------|---|--------|--------|-------|-------|-------|------|-------|-------|-------|--------|---|
| 10mm | 0 | -0,125 | -0,375 | -0,25 | -0,75 | -0,25 | 0,25 | -0,75 | -0,75 | -0,25 | -0,125 | 0 |

421
 422
 423 The same rotation history of Test 1 was then applied to the strengthened vault. At each rotation reversal
 424 step, the test was paused to allow surveying of the measuring rods, as well as the possible crack pattern,
 425 while the LVDTs system continuously captured the deformation of the vault profile. Test 2 was also stopped
 426 due to exceedance of the maximum rotation capacity of the testing bench.

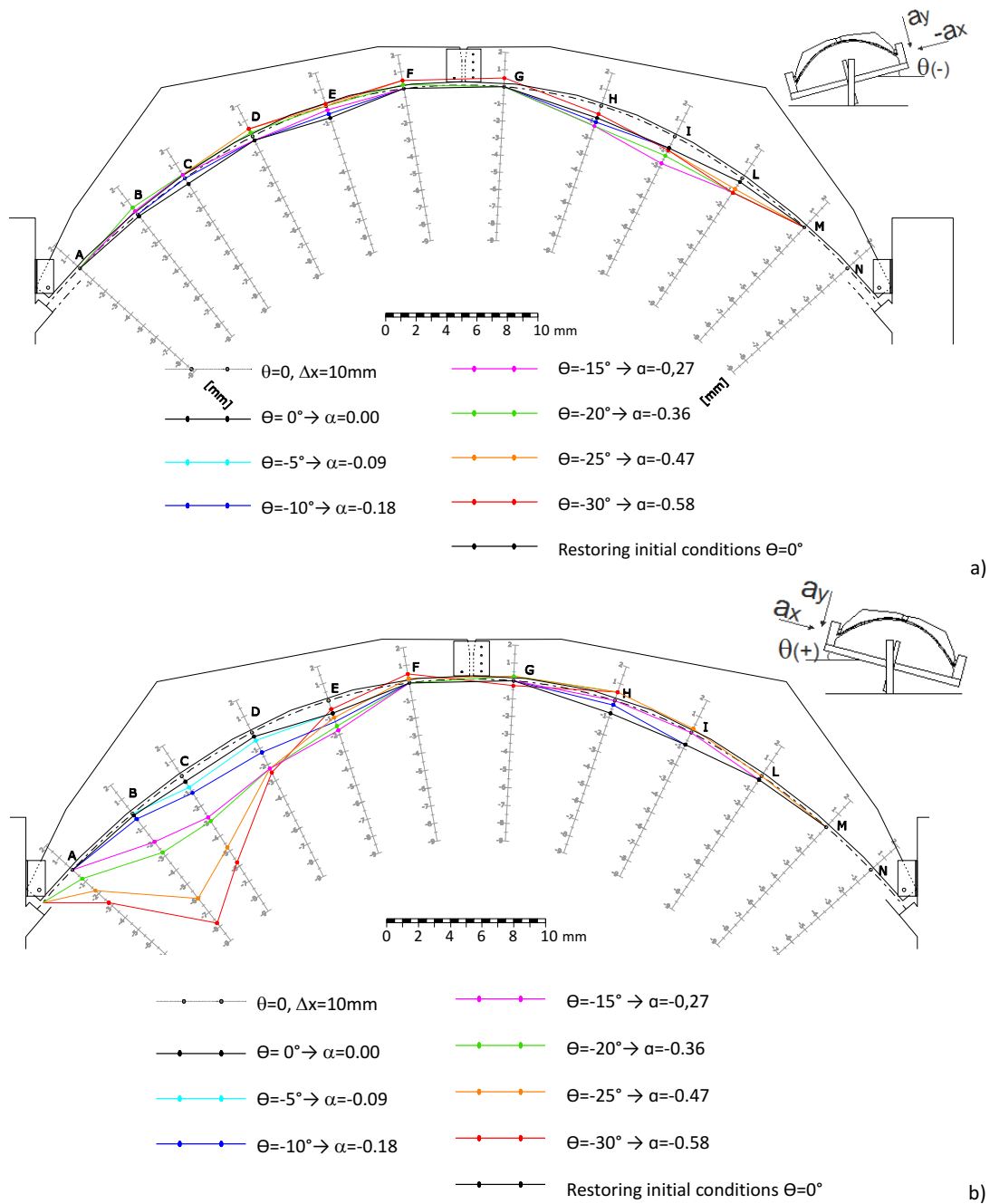
427 Figure 14a shows the vault and extrados centering maintaining contact at the key and springing sections
 428 throughout the entire counterclockwise rotation cycle. The leeward vault portion (segment B-C-D-E) tends
 429 to move closer to the reinforcement with increasing inclination, recovering the detachment resulting from
 430 the application of the horizontal relative displacement at the abutments. Contact is restored at a tilt of
 431 about -20° , thereby for acceleration ratio $\alpha = -0.36$. At the maximum inclination ($\theta = -30^\circ$), upward contact
 432 actions are exerted by the vault on the strengthening structure. Simultaneously, the windward segment of
 433 the vault (segment H-I-L-M) progressively detaches from the reinforcement up to an inclination of -15° ($\alpha =$
 434 0.27), with an average of about 1.5 mm and a maximum detachment of nearly 2mm at point I (Figure 13a).
 435 Beyond -15° rotations, the trend is reversed and the gap decreases; such a response is due to the upward

436 thrust applied by the vault (downward restraining action) at points B, C, D, E, F, resulting in an upward
437 displacement at points H, I, L. When the rotation angle is decreased from $\theta = 30^\circ$ to 0° , the vault and
438 restraining structure shift back to their initial position (Initial condition being: $\theta = 0^\circ$, $\Delta x = 10\text{mm}$). No
439 permanent displacements are measured. Cracks first develop at the key and springing sections at deck
440 rotations of about $\theta=20^\circ\div 25^\circ$; crack widths are at most equal to the tenth of a millimetre for $\theta=30^\circ$, and
441 close when restoring the initial conditions. Table 3 shows the relative displacements between the
442 restraining structure and the vault extrados as measured during counter-clockwise rotation.

443 A similar behaviour is observed in the case of clockwise rotations applied to the strengthened vault (Figure
444 14b). The abnormal relative displacements recorded in points A, B, C, D are caused by a local additional
445 clockwise rotation of the left abutment. Such a local rotation has a maximum value of 2° when the deck
446 approaches the rotation capacity of the testing bench, and disappears when the initial conditions are
447 restored. The local rotation of the abutment is caused by the impairment of the base restraint of the
448 abutment following the revision of the testing frame to allow for the application of the horizontal
449 settlement, and results in slight undesired indirect bending of the vault crown. Abnormal relative
450 displacements in points A, B, C, D are clearly visible for global rotations larger than $\theta > 20^\circ$ ($\alpha > 0,36$), and
451 maximum at $\theta \cong 30^\circ$, when 8mm detachment is observed in point B. Such a results shows that although the
452 contact between the vault and the strengthening structure is partly lost as a consequence of the possible
453 relative horizontal displacement of the abutments, the reinforcing element still exerts its restraining
454 function and contains the flexural deformations of the vault in the case of a seismic event. Table 4 shows
455 the relative displacements between the restraining structure and the vault extrados as measured during
456 clockwise rotation.

457 Figure 15 shows the maximum deformation of the vault at both clockwise and counterclockwise peak
458 rotations, measured through the LVDTs system (Fig. 5b). It is worth noting that the deformed shapes are
459 not symmetrical because of the unexpected local rotation of the left abutment observed while applying the
460 clockwise rotation. The hairline crack patterns are displayed in Figure 16. Throughout the test, no direct

461 bending failure mechanism was activated. As in Test 1, displacements were small throughout the test and
 462 compatible with the conservation of possible frescoes and stuccos.



464
 465 Figure 14 – Maximum relative displacements between the centering and the vault extrados during a) counterclockwise and b)
 466 clockwise rotations (displacements are magnified 100 times, see also Table 3 and 4).
 467

468
469

Table 3. Relative displacements (in mm) between restraining structure and the vault extrados as measured during counterclockwise rotation

| θ | A | B | C | D | E | F | G | H | I | L | M | N |
|----------|---|--------|-------|-------|-------|-------|------|-------|--------|-------|--------|---|
| -30 | 0 | 0,375 | 0,25 | 0,5 | 0,125 | 0,25 | 0,75 | -0,5 | -0,875 | -1 | -0,125 | 0 |
| -25 | 0 | 0,375 | 0,25 | 0,5 | 0 | 0,25 | 0,75 | -0,5 | -0,875 | -0,75 | -0,125 | 0 |
| -20 | 0 | 0,375 | 0,25 | 0,25 | 0 | 0 | 0,25 | -1,25 | -1,25 | -1 | -0,125 | 0 |
| -15 | 0 | 0,125 | 0,25 | -0,25 | -0,25 | -0,25 | 0,25 | -1,25 | -1,75 | -1 | -0,125 | 0 |
| -10 | 0 | -0,125 | 0 | -0,25 | -0,5 | -0,25 | 0,25 | -1 | -0,75 | -0,25 | -0,125 | 0 |
| -5 | 0 | -0,125 | -0,25 | -0,25 | -0,75 | -0,25 | 0,25 | -0,75 | -0,75 | -0,25 | -0,125 | 0 |

470

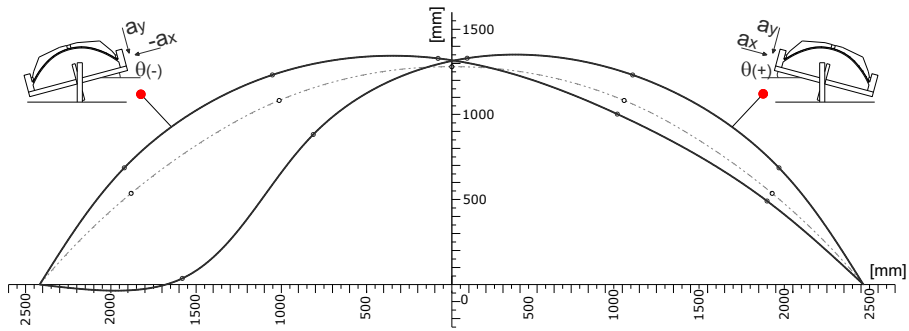
471
472

Table 4. Relative displacements (in mm) between restraining structure and the vault extrados as measured during clockwise rotation

| θ | A | B | C | D | E | F | G | H | I | L | M | N |
|----------|-------|--------|--------|-------|-------|-------|------|-------|-------|-------|--------|---|
| 5 | 0 | -0,125 | -0,75 | -0,5 | -0,75 | -0,25 | 0,25 | -0,75 | -1 | -0,25 | -0,125 | 0 |
| 10 | 0 | -0,5 | -1,125 | -1,25 | -1,25 | -0,25 | 0,25 | -0,25 | -0,75 | -0,25 | -0,125 | 0 |
| 15 | 0 | -2,125 | -2,75 | -2,25 | -1,75 | -0,25 | 0,25 | 0 | 0 | -0,25 | -0,125 | 0 |
| 20 | -0,75 | -2,875 | -3 | -2,25 | -1,5 | -0,25 | 0,5 | 0,5 | 0,25 | 0 | -0,125 | 0 |
| 25 | -1,75 | -6,125 | -4,75 | -2,25 | -1 | 0 | 0,5 | 0,5 | 0,25 | 0 | -0,125 | 0 |
| 30 | -2,75 | -7,875 | -5,75 | -2,5 | -0,5 | 0,25 | 0 | 0,5 | 0,25 | 0 | -0,125 | 0 |
| 0 | 0 | -0,125 | -0,375 | -0,25 | -0,75 | -0,25 | 0,25 | -0,75 | -0,75 | -0,25 | -0,125 | 0 |

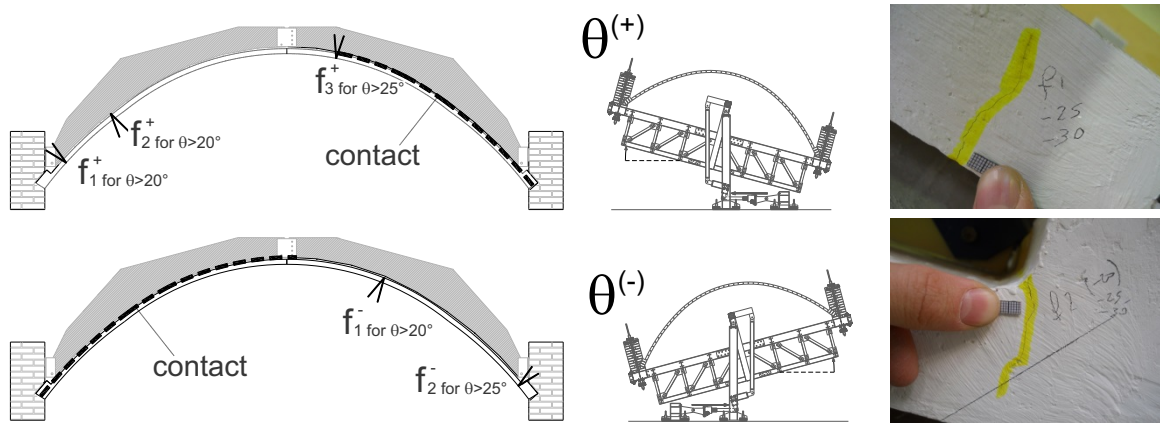
473

474



475
476
477

Figure 15 – Maximum deformed shape for counterclockwise and clockwise rotations (displacements are magnified 100 times).



478
479

Figure 16 – Schematic representation of crack location.

480

5. Concluding remarks

481

Traditional global retrofit interventions aimed at triggering the box-like seismic response of existing

482

buildings, including perimeter ties and floor and roof diaphragms, may be ineffective in inhibiting other

483 local failure mechanisms. In the case of existing structures with vaults, such global interventions cannot
484 prevent the onset of direct differential bending of any masonry vaults, induced by the inertia forces
485 associated the pertaining masses acting as a uniformly distributed horizontal load along the vault crown. In
486 the case of single leaf vaults, the direct differential collapse mechanism can be triggered by earthquakes of
487 very low intensity, as repeatedly evidenced by recent earthquakes showing completely collapsed vaults in
488 buildings with negligible crack patterns elsewhere.

489 In this paper, focus is placed on thin barrel masonry vaults conceived as lightweight false ceilings, lacking
490 lunettes and extrados backfilling material, and thus solely withstanding their self-weight. Such a typology is
491 quite common in churches, where single leaf vaults frequently cover the main nave, the apse and the side
492 chapels.

493 Lightweight plywood restraining structures are proposed to delay or inhibit the onset of direct
494 differential bending. The restraining structures are designed to apply passive confinement to the vault
495 extrados. The reinforcement is conceived as a 3-hinged arch to allow the accommodation of possible small
496 relative displacements of the vault springing, which may follow the small deformation of internal ties or
497 roof box structure. The solution stems as a passive solution, in which confinement is provided only if
498 needed. No shear transfer along the vault-to-restraining structure interface is allowed in order to avoid
499 possible vault decompression, which may be particularly detrimental in seismic conditions. The proposed
500 extrados restraining structure technique is a dry and cost effective solution, whose assembly and
501 positioning does not require specialised labour. The shape of the restraining structures is usually tailored
502 based on the geometry of the existing vault; however, possible small irregularities of the vault extrados can
503 be compensated through positioning of thin wedges. The technique is consistent with the restoration
504 principles of durability, full reversibility, and minimal impairment of the structure's integrity.

505 An experimental study allowed the assessment of the effectiveness of the proposed technique; further
506 evidence emerged through comparison with the seismic response of a reference unreinforced single leaf
507 vault tested in a past research study. A special pivoting testing frame was conceived to replicate distributed

508 horizontal accelerations in a quasi-static way. The test was stopped due to exceedance of the rotation
509 capacity of the testing frame. Throughout the test the strengthened single leaf vault substantially
510 outperformed the bare vault behaviour in terms of both stiffness and strength. The extrados centering
511 inhibited the onset of the failure mechanism for all the explored tilting angles of the testing bench, up to
512 accelerations of around 4 times greater than the acceleration triggering early failure of the unstrengthened
513 vault. At such accelerations, further mechanisms and different structural elements may be critical for the
514 existing building. It is worth noting that a significant increase in the structure stiffness was also observed,
515 which entails smaller displacements of the structure. Reduced maximum displacements are beneficial for
516 the preservation of possible stuccos or frescoes on the vault intrados.

517 An additional test was carried out to assess the effectiveness of the strengthening in the case of
518 loosening of possible intrados ties; in this case, a horizontal relative displacement of the abutment was
519 applied. The effectiveness was confirmed and also in this case the test was stopped due to exceedance of
520 the rotation capacity of the testing frame. Although the contact between the vault and the strengthening
521 structure was partly lost as a consequence of the applied horizontal displacement, the reinforcing element
522 still exerted its restraining function and contained the flexural deformations of the vault up to significant
523 tilting angles.

524 **6. Acknowledgments**

525 This work was financed and developed within the research project DPC-ReLUIS 2009-2012 – Research line
526 n.1. The authors thankfully acknowledge Luca Ferrario and Lorenzo Filippini for carrying out test n. 0-1 and
527 2, respectively; and express their appreciation to the technical staff of the Structural Testing Facility at the
528 University of Brescia for their assistance in the test program.

7. References

- 530 [1] Gulli, R., 1993, *Le volte in folio portanti: tecnica costruttiva ed impiego nell'edilizia storica e moderna*,
531 in: *Proceedings of "I° Convegno Nazionale Manutenzione e Recupero nella città storica"*, Rome (Italy).
532 ARCO (In Italian).
- 533 [2] Gulli, R. & Mochi G., 1995, *"Bóvedas tabicadas: architettura e costruzione"*, in: *"Il modo di costruire"*,
534 CDP editrice (In Italian).
- 535 [3] Ochsendorf, J. & Freeman, M. (photographs), 2010, *"Guastavino vaulting: the art of structural tile"*,
536 New York: Princeton Architectural Press.
- 537 [4] Ramage, M., Ochsendorf, J., Block, P. & Rich, P., 2008, *"Advanced Geometry, Rudimentary
538 Construction: Structural Form Finding for Unreinforced Thin-shell Masonry Vaults"* in *Advances in
539 Architectural Geometry 2008*, Vienna, Austria
- 540 [5] Gelfi, P. & Capretti A. 2001. *"Backfill role on the stability of arches and vaults"* pp.295-305. In:
541 *Structural studies, repairs, and maintenance of historical buildings VII*. Southampton : WIT Press.
- 542 [6] Heyman, 1966, *"The stone skeleton"*, *International Journal of Solids and Structures* 2, 249-279.
- 543 [7] O'Dwyer, D., 1999, *"Funicular analyses of masonry vaults"*, *Computer & Structures*, 73: 187-197.
- 544 [8] Block, P., DeJong, M. & Ochsendorf, J., 2006, *"As hangs the flexible line: Equilibrium of masonry
545 arches"*. *The Nexus Network Journal* 8 (2), pp. 13-24.
- 546 [9] D'Ayala, D. and Tomasoni, E. 2008. *The structural behaviour of masonry vaults: Limit state analysis
547 with finite friction*. *Proceedings of the VI International Conference on Structural Analysis of Historical
548 Constructions SAHC*. 2-4 July, Bath, England. pp. 47-71. Ed. Taylor and Francis, London, UK.
- 549 [10] Robertson, D., 1999, *"Seismic considerations for Guastavino ceiling, vault, and dome construction"*,
550 *APT Bulletin* Vol. 30, N. 4, p. 51-58.
- 551 [11] Ramaglia, G., Lignola, G.P., Prota, A., 2016. *Collapse analysis of slender masonry barrel vaults*.
552 *Engineering Structures*, Vol. 117, Pages 86–100
- 553 [12] Ochsendorf, J., 2006, *"The masonry arch on spreading supports"*, in *Structural Engineer* 84(2):29-35

- 554 [13] Giuriani, E. & Marini, A., 2008a “Experiences from the Northern Italy 2004 earthquake: vulnerability
555 assessment and strengthening of historic churches”, Proceedings of the VI International Conference on
556 Structural Analysis of Historical Constructions SAHC. 2-4 July, Bath, England. pp. 13-24. Ed. Taylor and
557 Francis, London, UK.
- 558 [14] Giuriani, E., Marini, A., Porteri, C. & Preti, M., 2009 “Seismic vulnerability of churches associated to
559 transverse arch rocking”, International Journal of Architectural Heritage, 3: 1–24, 2009. Ed. Taylor &
560 Francis Group, LLC.
- 561 [15] Giuriani, E. & Marini, A., 2008b, “Wooden roof box structure for the anti-seismic strengthening of
562 historic buildings”, Journal of Architectural Heritage: Conservation, Analysis and Restoration, Vol.2(3)
563 pp. 226-246.
- 564 [16] Ferrario, L., Marini, A., Riva, P. & Giuriani, E., 2010a, “Proportioning criteria for traditional and
565 innovative Extradados techniques for the strengthening of barrel vaulted structures subjected to rocking
566 of the abutments”, Journal of Civil Engineering and Architecture, David Publishing Company, USA,
567 pp.1-15. Vol. 4, N.5, May 2010.
- 568 [17] Oppenheim, IJ. 1992. The masonry arch as a four-link mechanism under base motion. Earthquake
569 engineering and Structural Dynamics 21(11):1005-1017.
- 570 [18] Ferrario, L., Marchina, E., Marini, A., Preti, M. & Giuriani, E., 2010b, “Lightweight ribs for the
571 strengthening of single-leaf vaults undergoing seismic actions”, Proceedings of the VIII International
572 Conference on Structural Analysis of Historical Constructions, Published in Advanced Materials
573 Research, Vol.133-134, pp.923-928. Ed. Xianglin Gu and Xiaobin Song, China.
- 574 [19] Ferrario, L., 2013, “Masonry single-leaf barrel vaults: from the seismic vulnerability assessment to the
575 proposal of an innovative retrofitting approach”, Ph.D. Thesis, University of Brescia.
- 576 [20] Tomasoni, E., 2008, “Le volte in muratura negli edifici storici, Tecniche costruttive e comportamento
577 strutturale”, Ph.D dissertation, University of Trento (In Italian).
- 578 [21] Giuriani, E., Gubana, A., & Arengi, A., 1999, Backfill and spandrel to limit the vault bending, Proc.
579 Strema 1999, Ed. Brebbia, Jager, Southampton, Boston, pp. 739-748.

- 580 [22] Ferrario, L., Marini, A., Riva, P. & Giuriani, E., 2009, "Traditional and Innovative Techniques for the
581 Seismic Strengthening of Barrel Vaulted Structures Subjected to Rocking of the Abutments", ATC-SEI
582 Conference on Improving the Seismic Performance of Existing Buildings and Other Structures. San
583 Francisco, California, December 9 -11.
- 584 [23] Valluzzi, M., Valdemarca, M. & Modena, C., 2001, "Behavior of Brick Masonry Vaults Strengthened by
585 FRP Laminates." *Journal on Composite Construction*, 10.1061/(ASCE)1090-0268(2001)5:3(163), 163-
586 169.
- 587 [24] Girardello, P., Pappas A., da porto F., Valluzzi, M.R., 2013, "Experimental testing and numerical
588 modelling of masonry vaults". International Conference on Rehabilitation and Restoration of
589 Structures, Chennai, 13-16 February 2013
- 590 [25] Giamundo, V., Lignola, G. P., Maddaloni G., Da Porto, F., Prota, A., Manfredi, G., 2016, "Shaking table
591 tests on a full-scale unreinforced and IMG retrofitted clay brick masonry barrel vault", *Bull Earthquake*
592 *Eng* 14:1663–1693; DOI 10.1007/s10518-016-9886-7
- 593 [26] Giamundo V., Lignola G.P., Maddaloni G., Manfredi G., 2015, "Experimental investigation of the
594 seismic performances of IMG reinforcement on curved masonry elements". *Compos Part B, Eng* 70:53–
595 63. doi:10.1016/j.compositesb.2014.10.039
- 596 [27] Ferrario, L., Marini, A., Andreis, V., Zanotti, S., Riva, P., Giuriani, E., 2012, "Behavior and retrofitting of
597 single-leaf vaults under distributed horizontal forces". In *Structural Analysis of Historical Construction*,
598 edited by Jerzy Jasienko, ed. Dolnoslaskie Wydawnictwo Edukacyjne DWE, Wroclaw, Poland, ISSN
599 0860-2395, ISBN 978-83-7125-216-7, Vol. 2, pp. 1503-1511.
- 600 [28] Marini A., Giuriani E., Ferrario L., Belleri A. & Preti M., 2015, "Indagini sperimentali sul rinforzo di volte
601 in folio con costolature lignee estradossali, effetto degli spostamenti delle imposte", Report
602 82_WP1_3-1c_UNIBG, Reluis research project DPC-ReLUIS 2014-2016 – Research line n.1.
- 603 [29] Marini, A., Giuriani, E., Belleri, A., Preti, M., Ferrario, L., 2016, "Plywood extrados retaining structures
604 for the retrofit of single leaf vaults", in: *Proc. Of 16th International Brick and Block Masonry*
605 *Conference "Masonry in a world of challenges"*, June 26 - 30, Padova, Italy. (In press).